

The temperature and composition of the mantle sources of Martian basalts

Max Collinet¹, Ana-Catalina Plesa¹, Thomas Ruedas^{2,1}, Sabrina Schwinger¹,
and Doris Breuer¹

¹German Aerospace Center (DLR), Institute of Planetary Research, Rutherfordstraße 2, 12489 Berlin,

Germany

²Museum für Naturkunde Berlin, Impact and Meteorite Research, Invalidenstraße 43, 10115 Berlin,

Germany

Key Points:

- Basalts that sampled discrete mantle regions throughout Mars's history provide information about the mantle composition and temperature
- The mantle potential temperature of primitive basalts appears constant (1400–1500 °C), yet is likely not representative of the average mantle
- Incompatible element concentrations in the mantle vary due to magma ocean crystallization, partial melting and metasomatism

Abstract

The composition of basaltic melts in equilibrium with the mantle can be determined for several Martian meteorites and in-situ rover analyses. We use the melting model MAGMARS to reproduce these primary melts and estimate the bulk composition and temperature of the mantle regions from which they originated. We find that most mantle sources are depleted in CaO and Al₂O₃ relative to models of the bulk silicate Mars and likely represent melting residues or magma ocean cumulates. The concentrations of Na₂O, K₂O, P₂O₅ and TiO₂ are variable and often less depleted, pointing to the re-fertilization of the sources by fluids and low-degree melts, or the incorporation of residual trapped melts during the crystallization of the magma ocean. The mantle potential temperatures of the sources are 1400–1500 °C, regardless of the time at which they melted and within the range of the most recent predictions from thermochemical evolution models.

Plain Language Summary

Martian meteorites and rocks analyzed by rovers are witnesses of magmatic processes on Mars. In this study, we use the mantle melting model MAGMARS to determine the composition and temperature of the mantle regions from which primitive basalts have originated. Primitive basalts are closely related to mantle melts and hence record the properties of their mantle source. We find that the mantle compositions needed to explain these melts were poor in CaO and Al₂O₃. They likely represent a mantle that melted on several occasions or that crystallized from an early magma ocean. The composition of these primitive basalts indicates that some elements (Na₂O, K₂O, P₂O₅ and TiO₂) were subsequently added to the mantle source by fluids and low-degree melts. Alternatively, these elements can be explained by the trapping of melts during the evolution and progressive crystallization of the magma ocean. The temperature of the mantle sources projected to the surface conditions for easier comparison, (i.e., potential temperature) was 1400–1500 °C, regardless of the time at which these sources melted and is within the range of the most recent predictions from planetary-scale models of interior dynamics.

1 Introduction

Our knowledge of the thermal state, composition and structure of the Martian mantle is derived from a diverse and continuously expanding array of geophysical and geochemical constraints. Early measurements of the moment of inertia factor, soil compositions at the Viking landing sites, and the definitive recognition that the “SNC meteorites” are from Mars (Baird et al., 1976; Johnston & Toksöz, 1977; Bogard & Johnson, 1983), unequivocally pointed to a FeO-rich mantle ($Mg/(Fe+Mg) \times 100$ in moles or Mg# = 75–81) compared to Earth (90). Model compositions of the “primitive mantle” were rapidly put forth (e.g., Dreibus & Wänke, 1985) and allowed to create simple models of the Martian interior structure (Longhi et al., 1992; Bertka & Fei, 1997; Elkins-Tanton et al., 2003). Additional analyses of crustal rocks by subsequent orbiting probes and rovers, the discovery of new Martian meteorites (Agee et al., 2013; Humayun et al., 2013), geodetic and seismic data from the recent InSight mission (e.g., Khan et al., 2021; Huang et al., 2022), and geodynamic modeling (e.g., Plesa et al., 2022), are now allowing to draw ever improving representations of the interior structure of Mars and its evolution through time.

Currently available compositions of the Martian mantle (e.g., Dreibus & Wänke, 1985; Lodders & Fegley, 1997; Yoshizaki & McDonough, 2020; Khan et al., 2022, abbreviated as DW85, LF97, YM20 and K22 hereinafter) represent average and idealized primitive compositions that are useful to derive average characteristics (density, solidus temperature, seismic wave velocity, etc.) but that probably do not represent actual regions of the mantle. The study of Martian meteorites has long shown that the mantle is highly

66 heterogeneous—both in terms of isotopic composition and Mg#—and suggests that a
 67 significant portion of the crust was formed very early (20–100 Myr; e.g., Borg et al., 1997;
 68 Debaillé et al., 2008; Humayun et al., 2013; Nyquist et al., 2016; Kruijer et al., 2017; Bou-
 69 vier et al., 2018) during (or briefly after) the crystallization of a Martian Magma Ocean
 70 (MMO). However, the major-element composition of the mantle reservoirs formed dur-
 71 ing the early differentiation of Mars is poorly constrained and model-dependent (e.g.,
 72 Borg & Draper, 2003; Elkins-Tanton et al., 2005).

73 To derive more detailed models of the interior structure of Mars, independent con-
 74 straints on the composition and temperature of discrete regions of the Martian mantle
 75 are desirable. A subset of Martian basalts, characterized by varied crystallization ages
 76 and high Mg# have been suggested to represent primitive basalts in near-equilibrium
 77 with their mantle sources and have been used to determine the P – T conditions of their
 78 mantle source through experiments (Musselwhite et al., 2006; Mondes et al., 2007; Fil-
 79 iberto et al., 2008; Filiberto, Dasgupta, et al., 2010; Filiberto, Musselwhite, et al., 2010)
 80 or modeling (Lee et al., 2009; Filiberto & Dasgupta, 2011, 2015; Filiberto, 2017; Bara-
 81 toux et al., 2011; Balta & McSween, 2013a). Most of these basalts cannot be produced
 82 by melting the primitive mantle and are instead expected to derive from mantle sources
 83 of diverse compositions (e.g., Schmidt & McCoy, 2010; Collinet et al., 2015, Fig. 1).

84 Here, we use MAGMARS, a new model developed to simulate melting in the Mar-
 85 tian mantle (Collinet et al., 2021), to re-evaluate the melting conditions and the ther-
 86 mal state of the mantle sources of primitive Martian basalts, which crystallized at dif-
 87 ferent times and therefore represent snapshots of Mars' thermochemical evolution. In
 88 addition, MAGMARS allows us to estimate for the first time the major-element com-
 89 position of these local mantle sources. We find that the P – T melting conditions appear
 90 to have remained relatively stable through time and that mantle sources display vari-
 91 able CaO/Al₂O₃, low overall abundances of incompatible elements but enrichment of al-
 92 kalis, P and Ti relative to Ca and Al. We discuss the implications of these findings for
 93 the early differentiation of Mars and its long-lived magmatism.

94 2 Selected compositions of primitive Martian basalts

95 While the majority of mantle melts were modified by igneous differentiation as they
 96 ascended through the crust (Udry et al., 2018; Payré et al., 2020; Ostwald et al., 2022;
 97 Farley et al., 2022; Wiens et al., 2022), a limited number of Martian basalts bear wit-
 98 ness to the composition and temperature of the mantle at the time of their formation
 99 (i.e., primitive basalts). To identify primitive basalts, we first make the assumption that
 100 the average Martian mantle contains olivine Mg# ≥ 77 (Table 1, Table S1 and Fig. 1),
 101 and would produce primary melts with a Mg# ≥ 54 ($K_{D, \text{Fe-Mg}}^{\text{oliv-liq}}$ of 0.35; Filiberto & Das-
 102 gupta, 2011). A mantle of Mg# 77 is intermediate between the most commonly accepted
 103 primitive mantle compositions (Dreibus & Wänke, 1985; Yoshizaki & McDonough, 2020).
 104 Here, we only consider martian basaltic compositions with a Mg# ≥ 48 , which could de-
 105 rive from primary mantle melts of Mg# ≥ 54 following a maximum of 10 wt.% of olivine
 106 fractionation.

107 The Spirit rover analyzed numerous basalts with Mg# 48–55 at Gusev crater (McSween,
 108 Wyatt, et al., 2006; Squyres et al., 2007; Ming et al., 2008) that could represent prim-
 109 itive basalts (Mondes et al., 2007; Filiberto, Dasgupta, et al., 2010; Schmidt & McCoy,
 110 2010). Among these, the Adirondack-class basalts are poor in K₂O and could derive from
 111 a residual mantle depleted in incompatible elements by prior melting events (Schmidt
 112 & McCoy, 2010; Collinet et al., 2021) while most of the basalts analyzed in the vicin-
 113 ity of the Columbia Hills are more enriched in alkali elements and poorer in CaO (Fig.
 114 1). The ancient regolith breccia NWA 7034/7475/7533 (Humayun et al., 2013; Nyquist
 115 et al., 2016; Cassata et al., 2018; Bouvier et al., 2018) is also characterized by a high Mg#
 116 (54; Wittmann et al., 2015) and, despite its complex history, could approach the com-

position of a mantle melt based on trace (Humayun et al., 2013) and major element compositions (Collinet et al., 2015). We also test whether two individual clasts could be representative of primitive basalts later remelted by impacts: a vitrophyre (Udry et al., 2014) and an alkali-rich microbasalt known as “Clast VI” (Humayun et al., 2013).

Recent geophysical constraints suggest that large portions of the mantle could be more Mg-rich ($Mg\# = 81$; Khan et al., 2022) than previously assumed (e.g., Dreibus & Wänke, 1985; Yoshizaki & McDonough, 2020), as also evidenced by the study of Martian meteorites. The most primitive depleted shergottite (Yamato 980459, nearly identical to NWA 5789; Greshake et al., 2004; Gross et al., 2011) and the most primitive enriched shergottite (LAR 06319, nearly identical to NWA 1068; Barrat et al., 2002; Pessler et al., 2010) have $Mg\#$ of 66 and 58, respectively. Y 980459 contains olivine $Mg\#$ 85–86 and is thought to represent a primary melt composition (e.g., Musselwhite et al., 2006; Matzen et al., 2022). The olivine megacrysts in LAR 06319 and NWA 1068 have $Mg\# \leq 77$ (Basu Sarbadhikari et al., 2009) but were initially more magnesian ($Mg\# 80$) and were modified by Fe–Mg diffusion (Balta et al., 2013; Collinet et al., 2017). NWA 2737 is a dunitic cumulate ($Mg\# 79$) with olivine-hosted melt inclusions. Its primary melt is taken as the reconstructed composition of the parental trapped liquid (PTL; He et al., 2013). Given the multitude of evidence of Mg-rich mantle reservoirs, we also calculated alternative primary melt compositions for the Gusev basalts and NWA 7034/7475/7533 bulk rock and basaltic clasts that would be in equilibrium with a $Mg\#$ of 81. In this case, larger amounts of olivine have to be added to the parental melt compositions (Table 1).

Table 1. List of Martian primitive basalts, fraction of olivine addition required to reach mantle-melt equilibrium, and associated inferred mantle $Mg\#$

		age (Ga)	oliv (wt.%)	$Mg\#$
NWA 7034	Vitrophyre [1]	4.49 [2]	+10 / +26	77 / 81
NWA 7533	Clast VI [3]	4.49 [2]	+9 / +24	77 / 81
NWA 7475	bulk [4]	4.49 [2]	0	77
Adirondack-class basalts [5]		3.7 [6]	+3 / +17	77 / 81
Columbia Hills	Humboldt Peak [7]	3.7 [6]	+7 / + 20	77 / 81
	Fastball [8]	3.7 [6]	0 / +13	77 / 81
	Stars, etc. [8]	3.7 [6]	+5 / +17	77 / 81
	Ace [8]	3.7 [6]	+9 / +29	77 / 81
	Irvine [7]	3.7 [6]	+8 / +25	77 / 81
chassignite	NWA 2737 [9]	1.3 [10]	+9	79
depleted shergottite	Y 980459 [11]	0.47 [12]	0 / +7	85 / 86
enriched shergottite	LAR 06319 [13]	0.19 [14]	0 / +5	80 / 81

[1] Udry et al. (2014), [2] Costa et al. (2020), [3] Humayun et al. (2013), [4] Wittmann et al. (2015)

[5] McSween, Wyatt, et al. (2006), [6] Greeley et al. (2005), [7] Ming et al. (2008)

[8] Squyres et al. (2007), [9] He et al. (2013), [10] Udry and Day (2018)

[11] average of Misawa (2004), Shirai and Ebihara (2004) and Greshake et al. (2004)

[12] Shih et al. (2005), [13] Basu Sarbadhikari et al. (2009), [14] Shafer et al. (2010)

3 Methods

To constrain the mantle sources of the target basaltic compositions described above (Table 1 and S1), we first simulate the melting of various primitive mantle compositions (DW85, YM20 and K22) using MAGMARS (Collinet et al., 2021). We then adjust the mantle compositions incrementally ($Mg\#$, TiO_2 , Al_2O_3 , CaO , Na_2O , K_2O , and P_2O_5 concentrations) until the liquids produced are identical to the target compositions (i.e.,

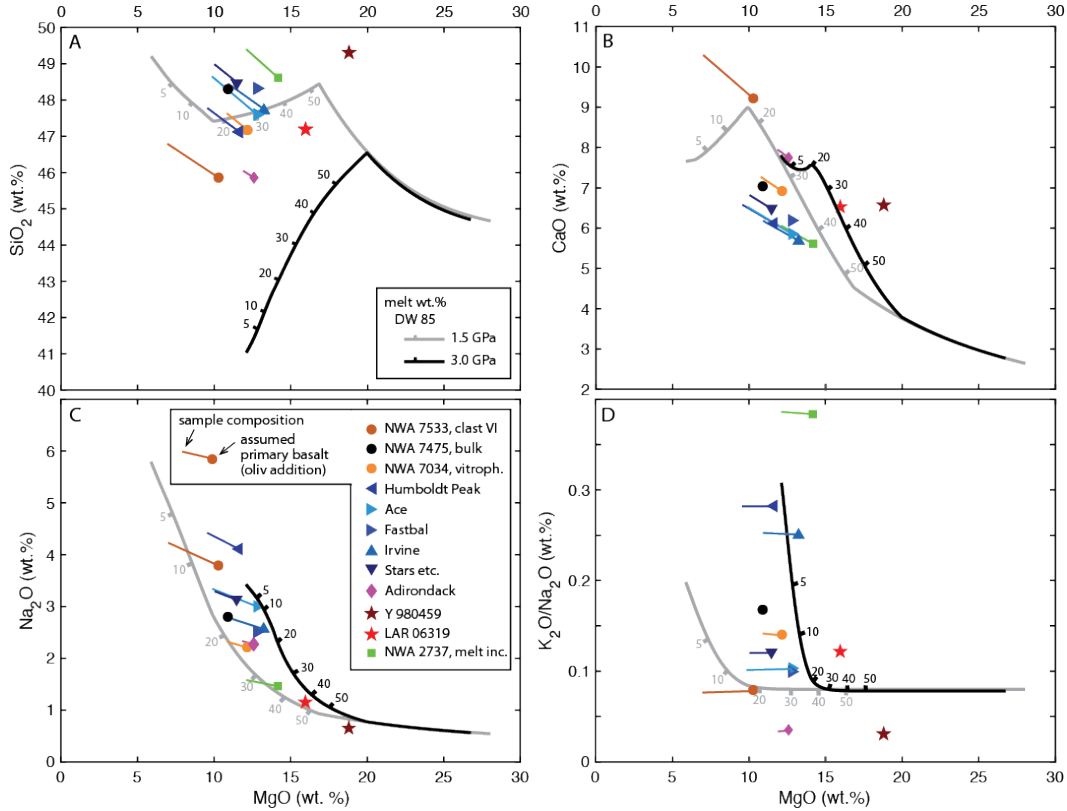


Figure 1. Comparison between the composition of Martian primitive basalts (left extremity of colored lines), their recalculated primary melts (symbols) and the melts produced by melting of the primitive mantle of Dreibus and Wänke (1985) at 1.5 (grey line) and 3.0 GPa (black line), as calculated by MAGMARS. The high SiO₂ content of primary melts (A) is consistent with shallow melting conditions ($\ll 3.0$ GPa). But compared to shallow DW85 melts (1.5 GPa), many primary basalts have either lower or higher CaO contents (B) and higher Na₂O and K₂O contents (C-D), and must therefore derive from mantle sources of contrasting compositions.

when the concentrations of all major and incompatible elements are within 1 wt.% relative). Next, we mathematically remove a fraction (33 to 50 wt.%) of the melt (of composition identical to the target compositions) and repeat the same procedure to identify more refractory mantle compositions that can still produce identical melts. This approach, in the absence of independent constraints on the melt fraction, leads to the identification of several possible mantle sources for each target composition. To discuss the non-uniqueness of the sources and quantify model uncertainties for the Fastball primary melt (representative example), we performed ~ 500000 MAGMARS calculations by randomly varying the parameters around their average values. This automated search identified slightly larger compositional trends compared to the manual search. However, the mantle sources identified manually were found sufficient to discuss the mantle source origin and melting temperature. It is this dataset (Table S2) that is described in the following sections.

4 Results

The compositions of the mantle sources that can produce melts identical to the target primary basalts (Table 1 and Fig. 1) are shown in Figure 2 and reported in Table S2. Each primary basalt composition can be matched by melting a series of mantle sources characterized by various concentrations of incompatible elements (Al_2O_3 , CaO , Na_2O , K_2O), both isobarically and polybarically. Despite the non-uniqueness of solutions, first-order chemical differences between the sources of the different basaltic compositions can be identified. For example, the possible sources of shergottites are all notably poorer in Al_2O_3 and Na_2O than the sources of the Gusev basalts (Fig. 2a). Among the latter, the sources of the Columbia Hills basalts are characterized by high Na_2O , K_2O , and P_2O_5 concentrations (Fig. 2b–d) compared to the source of the Adirondack basalts. The source of the NWA 2737 chassignite shows the highest $\text{K}_2\text{O}/\text{Na}_2\text{O}$ ratio. Finally, one of the sources that can match the composition of Clast VI (NWA 7533) is nearly identical to the DW85 primitive mantle.

The melt fractions required to produce the primary basalt compositions are comprised between 5 and 30 wt.%. The associated mantle potential temperatures (T_p) are between 1320 and 1520 °C (Fig. 3a and Table S2). The average pressure of melting is relatively low for all samples (1.1–2.0 GPa), and is largely constrained by the SiO_2 and MgO concentrations of the target primary melts (Fig. 1a). If a Mg# of 81 (K22) is assumed instead of 77 for NWA 7034/7475/7533 and Gusev basalts, then the primary basalts would contain a larger olivine component and the mantle T_p (1390–1570 °C) and average pressure of melting (1.9–3.0 GPa) would both be higher (Fig. 3).

5 Discussion

5.1 Thermal state of the Martian mantle

Compared to the T_p estimates of Filiberto (2017), and using the same starting assumptions (mantle of Mg# 77 and batch melting), we find that Gusev crater basalts are derived from slightly cooler mantle sources on average, with T_p of ~ 1400 °C (vs. ~ 1450 °C), but that the ranges of possible T_p largely overlap (1360–1460 vs. 1390–1550 °C, respectively). Allowing for a higher Mg# of the mantle sources (77–81), we find that Gusev basalts and all (pre-)Noachian to Hesperian samples point to a T_p of 1340–1520 °C (Fig. 3a).

We calculate a T_p of 1420–1430 °C for the primary melt composition reconstructed from NWA 2737 melt inclusions (He et al., 2013), assumed to be parental to the middle-Amazonian nakhlites and chassignites (1.34 Ga; Udry & Day, 2018). However, the mantle source could have been metasomatized (Day et al., 2018, also see section 5.2) and could

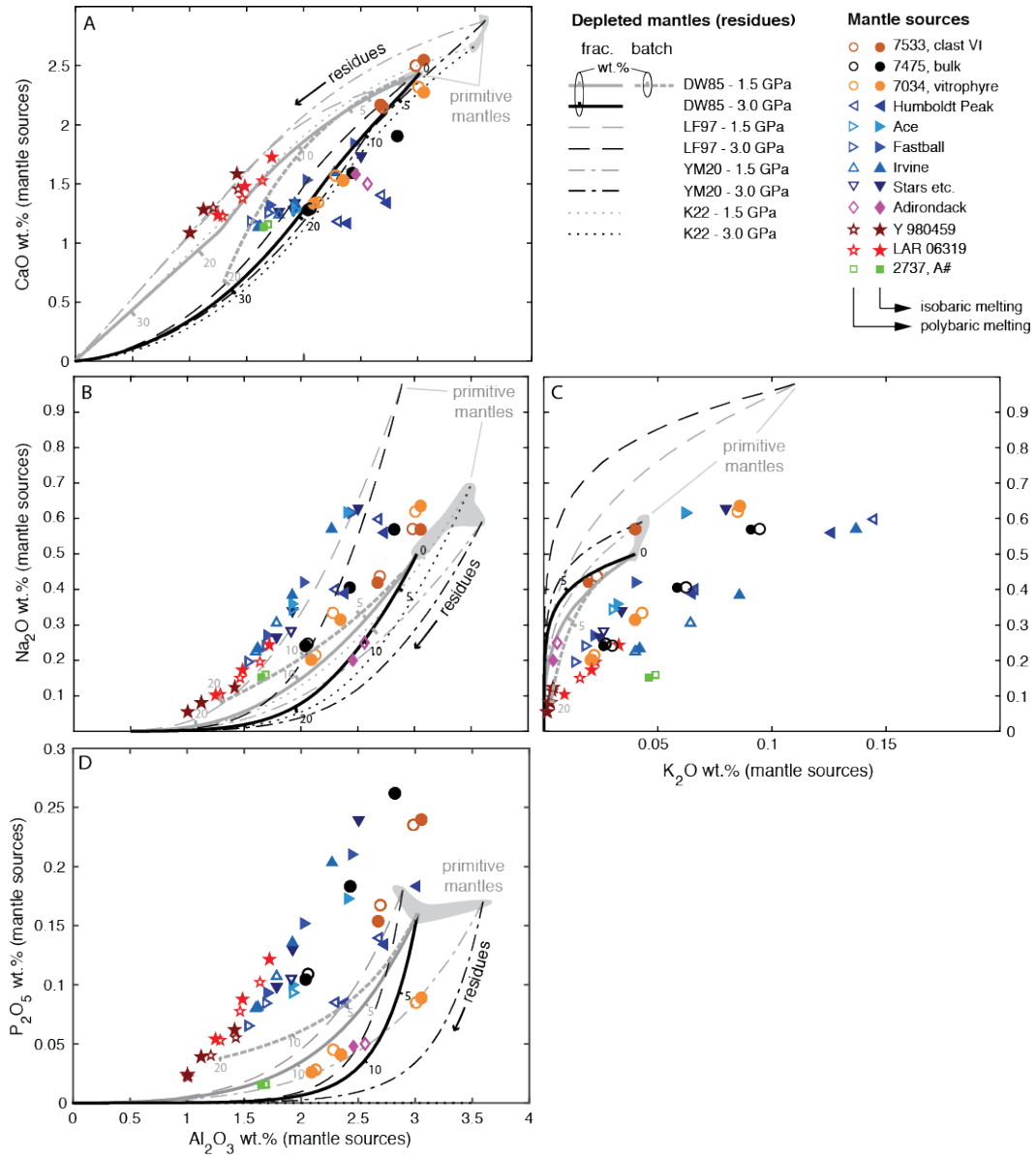


Figure 2. Incompatible element concentrations of the mantle sources of primary basalts (symbols) compared to residual model Martian mantles (lines). Each line represents the trajectory of residues produced by progressive melting of a primitive mantle composition (apex) at 1.5 (grey) and 3.0 GPa (black). For the DW85 model (solid lines), tick marks indicate the composition of residues after specific degrees of melting (in wt.%). All mantle source compositions are relatively poor in CaO and Al₂O₃ compared to the primitive mantle and are characterized by variable CaO/Al₂O₃ (A). The source of NWA 7533 clast VI is similar to a primitive mantle (DW85) and the source of the Adirondack basalts resemble a residual mantle following prior partial melting in all compositional spaces (A–D). All other sources are too rich in alkali elements—Na₂O (B) and especially K₂O (C)—and other incompatible elements, such as P₂O₅ (D), to derive from model Martian mantles by partial melting alone and other processes must be considered (see section 5.2).

have contained up to 250 ppm of water (McCubbin et al., 2016), which would translate into a lower T_p of 1380 °C (Katz et al., 2003).

The more recent olivine-phyric shergottites (160–500 Ma; Moser et al., 2013; Wu et al., 2021; McFarlane & Spray, 2022) are picritic basalts that have been linked to plumes with a T_p of at least 1480–1550 °C (e.g., Musselwhite et al., 2006; Filiberto & Dasgupta, 2015). The T_p of MAGMARS simulations (1470–1520 °C) are within error of these previous constraints if batch melting is assumed, and slightly lower in the polybaric case (1440–1450 °C). The presence of water in the source of shergottites could in principle lower the minimum T_p and has been suggested to account for their relatively high SiO₂ concentrations (Balta & McSween, 2013b). However, the small initial water concentration of the source (14–73 ppm; McCubbin et al., 2016) and the fact that the SiO₂ concentration of shergottite melts can be reproduced with MAGMARS under nominally anhydrous conditions preclude a significant effect of water.

Finally, we re-calculate using MAGMARS the T_p and pressures of melting of the bulk volcanic provinces of Baratoux et al. (2011), as constrained by the Gamma Ray Spectrometer (GRS) on board NASA's Mars Odyssey spacecraft. Baratoux et al. (2011) used pMELTS in their analysis, which has since been shown to overestimate FeO and underestimate SiO₂ concentrations by up to 8 wt.% (Collinet et al., 2021), significantly more than anticipated by El Maarry et al. (2009). For Hesperian provinces, while the ranges of T_p are similar (1390–1460 vs. 1370–1420 °C previously), MAGMARS predicts a slightly higher pressure of melting (1.6–2.3 vs. 1.3–1.6 GPa). However, we find that only Ascraeus and Elysium Mons (out of the 6 Amazonian volcanic provinces) can be matched with a DW85 mantle composition using MAGMARS (Table S3). The composition of the other 4 provinces can either not be reproduced at all (Arsia and Pavonis Mons) or only with an extremely small melt fraction of <2 wt.% (Olympus Mons and Alba Patera). With a YM20 composition (Mg# of 79, 81 after 15 wt.% of melting), a higher T_p of 1520–1660 °C and higher pressures of melting (2.3–3.5 GPa) are necessary to match the Hesperian volcanic provinces. A higher Mg# mantle also allows to reproduce the composition of a greater number of Amazonian volcanic provinces (5, all but Arsia Mons) with T_p of 1380–1460°C and pressures of 2.8–3.1 GPa.

The lack of temperature and pressure trends over time displayed by this set of constraints renders it impossible to calculate rates of secular cooling or lithosphere thickening (Fig. 3a,b). This could be due to the limited number of primitive basalts available that might not be representative of the average mantle. To test this possibility, we compare the mantle temperature estimates derived from MAGMARS to the results of a global convection model incorporating the most recent interior structure constraints from InSight (Plesa et al., 2022). The maximum temperature (and minimum pressure) at which the mantle is melting decreases with time (i.e. secular cooling). However, at any given time, melt is produced from regions of the mantle with highly variable T_p , which encompass the T_p of the mantle sources estimated in this study. The Gusev basalts are the only primitive basalts whose location is known with certainty. Additionally, NWA 7034 and the depleted shergottites have recently been suggested to have originated from Karratha and 09-000015 craters, respectively (Lagain et al., 2021, 2022). Under all three locations and at the appropriate—and highly contrasting—crystallization ages, the T_p of the mantle sources would have been nearly identical and in the range 1525–1562 °C (Fig. 3c,d and S3). This confirms that despite the overall decrease in mantle temperature with time, a limited basaltic sample suite can record near-constant mantle temperature. The thermochemical evolution model predicts that the mantle temperature should first increase due to the decay of radioactive elements and peak at the Noachian/Hesperian transition before slowly decreasing (e.g., Plesa et al., 2022). This thermal maximum is not recorded by the 3.7 billion years old Gusev basalts but seems consistent with our re-interpretation of the T_p of Hesperian volcanic provinces (1520–1660 °C; Baratoux et al.,

244 2011), assuming that the average mantle is relatively MgO-rich (Mg# of 79; Yoshizaki
 245 & McDonough, 2020).

246 Perhaps the main discrepancy between the thermochemical evolution model and
 247 the MAGMARS constraints is the shallow depth of melting that we estimate for the source
 248 of shergottites, which is predicted to be well within the lithospheric mantle (Plesa et al.,
 249 2022). Filiberto (2017) noted that if a larger amount of olivine fractionation had taken
 250 place, the primary melts of shergottites could have been in equilibrium with the convect-
 251 ing mantle at 3–5 GPa. While this pressure of melting is more consistent with the thick
 252 lithosphere of the late Amazonian (Fig. S3), such melt compositions would require a high
 253 T_p of 1710 ± 73 °C, which exceeds significantly the maximum T_p achievable by thermal
 254 evolution models at that time (Fig. 3d). Therefore, we consider it more likely that the
 255 T_p of the sources was low (1470–1520 °C) and that the pressure of melting derived from
 256 MAGMARS simulations (1.6 ± 0.5 GPa) does not represent the average pressure of melt-
 257 ing but simply the final pressure of equilibration with the mantle. If shergottites formed
 258 in the Tharsis region (e.g., Lagain et al., 2021), deeply-sourced primary melts could have
 259 re-equilibrated with a warm lithospheric mantle, locally heated by magmas, at the base
 260 of the crust (110–130 km; Wieczorek et al., 2022).

261 5.2 Origin of the mantle sources and their variable concentrations of in- 262 compatible elements

263 The mantle source of Clast VI (NWA 7533) could be nearly identical to the prim-
 264 itive mantle (Fig. 2), as previously suggested based on rare-earth element (REE) mod-
 265 eling (Humayun et al., 2013). All other mantle sources are depleted in CaO and Al₂O₃
 266 relative to the various primitive mantle compositions proposed in literature (DW85, LF97,
 267 YM20 and K22). One possibility is that these mantle sources represent melting residues
 268 from which 10–20 wt.% melt had been removed prior to producing the melts that even-
 269 tually formed the primitive basalts used in this study (Fig. 2a). However, the concen-
 270 trations of alkalis and other incompatible elements (e.g., TiO₂, P₂O₅) are, in most cases,
 271 too high at a given Al₂O₃ concentration, regardless of the style (batch vs. fractional) and
 272 pressure of melting (Fig. 2b–d). Only the Adirondack basalts are consistent in detail with
 273 the simple re-melting of a mantle residue, following ± 10 wt.% prior melting of a prim-
 274 itive mantle (see also Collinet et al., 2021). Other processes must be invoked to explain
 275 the chemical variability of the remaining mantle sources.

276 The Columbia Hills basalts are often assumed to be related to the Adirondack basalts,
 277 as both groups were analyzed by Spirit at Gusev crater. Compared to the Adirondack
 278 basalts, they are rich in alkali elements as well as other incompatible elements (TiO₂,
 279 P₂O₅) and poor in CaO and Al₂O₃ (Fig. 1). McSween, Ruff, et al. (2006) suggested that
 280 the Columbia Hills basalts could have derived from melts similar to the Adirondack basalts
 281 by fractional crystallization. The higher incompatible element concentrations (e.g., K,
 282 P, Ti) of the Columbia Hills basalts have also been suggested to result from the contam-
 283 ination of Adirondack-like primitive melts by a crustal component (Schmidt & McCoy,
 284 2010). However, crustal assimilation and fractional crystallization (AFC) of basaltic melts
 285 should lower markedly the MgO concentrations (and Mg#; Ostwald et al., 2022). As the
 286 Mg# of the Columbia Hills and Adirondack basalts are similar, most workers now re-
 287 gard them as two sets of near-primary melts (Schmidt & McCoy, 2010; Filiberto & Das-
 288 gupta, 2011; Collinet et al., 2015). Schmidt and McCoy (2010) proposed that the high
 289 K₂O content of the Columbia Hills basalts could be accounted for by melting a fertile
 290 mantle source with a higher K₂O content compared to the Dreibus and Wänke (1985)
 291 composition. According to their model, the Adirondack basalts would be slightly younger
 292 and produced by re-melting the same region of the mantle. However, the similarly low
 293 CaO and Al₂O₃ concentrations of their sources (Fig. 2a) suggest that both the Adiron-
 294 dack and Columbia Hills basalts were derived from depleted mantles, affected by 10–20
 295 wt.% prior melting at ~ 3.0 GPa. Metasomatism has been invoked to reconcile the high

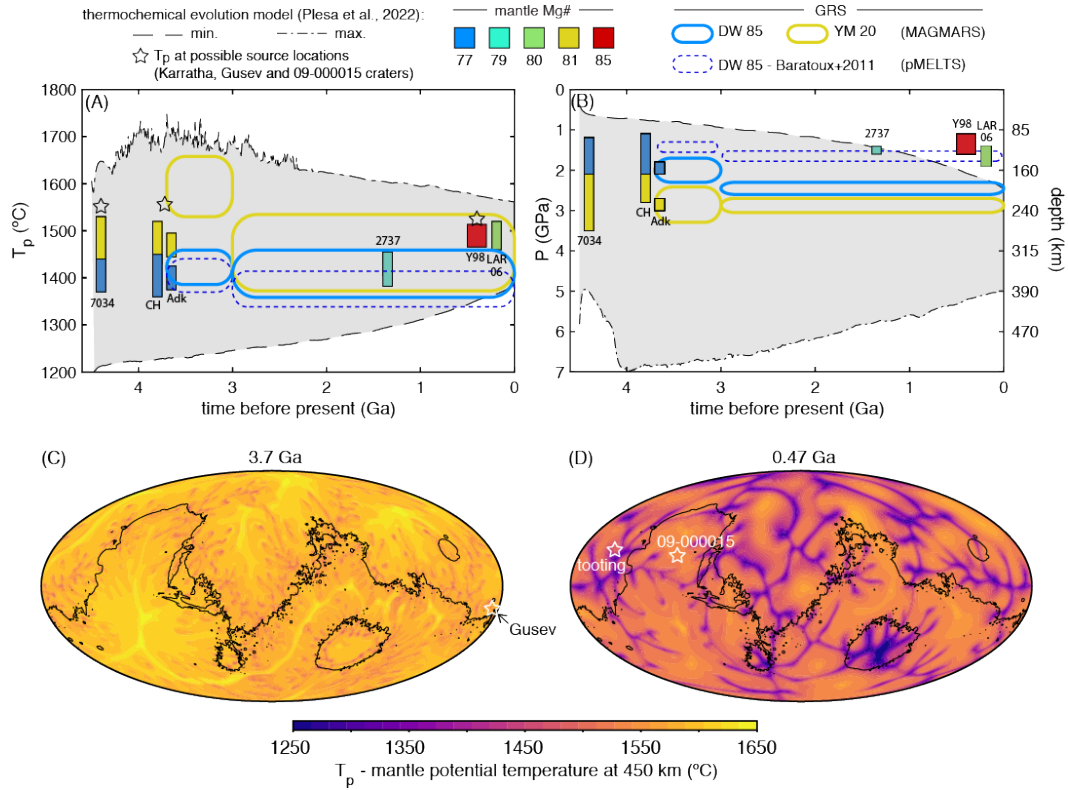


Figure 3. Temporal evolution of T_p (A) and the average pressure and depth of melting or conditions of mantle–melt re-equilibration (B). The rectangles represent the sources of the basaltic compositions listed in Table 1. The rounded fields are the sources of the GRS volcanic provinces of Baratoux et al. (2011), re-calculated with MAGMARS. The black lines represent the evolution of the potential temperatures and pressures of the part of the mantle that is affected by partial melting in the thick-crust geodynamical model of Plesa et al. (2022). The minimum pressure of melting (dashed line in B) can be interpreted as the thinnest thermal lithosphere observed anywhere on the planet. Panels C and D represent regional variations in T_p for this geodynamical model at the time of Gusev basalt (C) and depleted shergottites (D) crystallization. At their possible source locations (white stars, see text for references), the T_p are nearly identical: 1562 vs. 1525 °C (see also Fig. S3).

water and incompatible element concentrations of nakhlites-chassignites with their Sr-Nd isotopic compositions indicative of ancient depleted sources (Goodrich et al., 2013; McCubbin et al., 2013; Day et al., 2018) and could also help explain the high K₂O concentrations analyzed in numerous rocks from Gale crater (e.g., Schmidt et al., 2014). Similarly, we posit that the relative enrichment of incompatible elements in the Columbia Hills basalts (alkali elements as well as elements like P and Ti that are less mobile in fluids) could be explained by the secondary addition of low-degree melts to a Adirondack-like mantle source. The highest possible K₂O concentrations that we calculate for the Columbia Hills mantle sources are in the range 0.13–0.15 wt.%. This is much smaller than the percent level K₂O concentrations of highly metasomatized and phlogopite-bearing terrestrial peridotites (e.g., Condamine & Médard, 2014) but similar to other intraplate peridotites containing no hydrous phases (e.g., Smith et al., 1993). The source of the Columbia Hills basalts was likely affected by low degrees of cryptic metasomatism and was thus not significantly hydrated.

The isotopic systematics of Martian meteorites suggest the existence of a magma ocean that crystallized early in Mars' history (e.g., Elkins-Tanton et al., 2005; Debaille et al., 2008; Kruijer et al., 2017; Bouvier et al., 2018). Some of the resulting heterogeneity was never erased by convection and ancient mantle sources were affected by partial melting and formed the shergottites as recently as 170 million years ago (Moser et al., 2013; Wu et al., 2021; McFarlane & Spray, 2022). The major and incompatible element concentrations of the sources of shergottites must in part reflect the processes of magma ocean crystallization. For example, the superchondritic CaO/Al₂O₃ ratio of shergottites has been suggested to result from the fractionation of majorite in the deep mantle (Borg & Draper, 2003). Here, we find that the sources of shergottites had mildly superchondritic CaO/Al₂O₃ ratios that could have appeared at low pressure, following 15–20 wt.% melting of the primitive mantle (Fig. 2a). A 20 wt.% depletion from a primitive mantle is also sufficient to decrease the incompatible element concentrations to levels identical to those of the source of depleted shergottites (Fig. 2b–d). In this case, however, the melting residue only reaches a Mg# of 77 (when starting from a DW85 mantle) to 81 (YM20), following 20 wt.% of melting. The much higher Mg# of the source of Y 980659 (85–86) remains easier to explain if it formed as a magma ocean cumulate (e.g., Borg & Draper, 2003; Elkins-Tanton et al., 2005). The enriched shergottites have higher concentrations of incompatible elements. Their composition in radiogenic isotopes indicates that the enriched signature is most likely derived from evolved residual melts that were trapped in mantle cumulates during the crystallization of an early MMO, rather than from crustal assimilation (e.g., Borg & Draper, 2003; Symes et al., 2008; Debaille et al., 2008; Brandon et al., 2012; Ferdous et al., 2017; Armytage et al., 2018). This could also explain the slightly higher concentrations of minor incompatible elements that we calculate for the source of enriched shergottites (Fig. 2).

6 Conclusions

The mantle temperature of the sources that gave rise to known primitive basalts appears to have remained relatively stable through time (T_p of 1400–1500 °C). This could be due to a sampling bias. The higher mantle T_p (~1600 °C) of the Hesperian volcanic provinces (Baratoux et al., 2011), recalculated with MAGMARS and assuming a mantle with Mg# of 79 or higher (Yoshizaki & McDonough, 2020; Khan et al., 2022), hint at a significant secular cooling (>100 °C) as expected from thermochemical evolution models (Plesa et al., 2022). The shergottite melts were likely produced at pressures greater than 3 GPa but re-equilibrated with the lithospheric mantle at 1–2 GPa, for example at the base of the thick Tharsis crust.

With the exception of the source of NWA 7034 and paired rocks, the mantle sources of known Martian basalts were poorer in Al₂O₃ and CaO compared to primitive mantle compositions (e.g., Dreibus & Wänke, 1985; Yoshizaki & McDonough, 2020). The com-

348 positions of the sources of Gusev crater basalts that we calculate do not explicitly re-
 349 quire a magma ocean stage and could represent simple depleted mantle reservoirs affected
 350 by 10–20 wt.% prior melting (Adirondack basalts) or depleted mantle reservoirs re-fertilized
 351 by fluids and low-degree silicate melts (Columbia Hills basalts). On the other hand, the
 352 major element composition of the source of depleted shergottites cannot be easily ex-
 353 plained by partial melting alone and suggest, along with their Sr-Nd-Hf isotope system-
 354 atics, that they formed as mantle cumulates during the crystallization of the MMO. The
 355 sources of enriched shergottites are consistent with trapping a more evolved residual melt.
 356 It is also possible that the relative enrichment of the minor incompatible elements (Na,
 357 K, Ti and P) of the Columbia basalts is a vestige of magma ocean processes and does
 358 not result from metasomatism. But regardless of its origin, this relative enrichment is
 359 limited, with concentrations of Na₂O, P₂O₅, and TiO₂ not exceeding the range displayed
 360 by primitive mantle compositions.

361 Acknowledgments

362 M.C. and A.C.P. gratefully acknowledge the financial support and endorsement from the
 363 DLR Management Board Young Research Group Leader Program and the Executive Board
 364 Member for Space Research and Technology. M.C. and S.S. were supported by DFG (Deutsche
 365 Forschungsgemeinschaft) from the DFG programme SFB-TRR 170. T.R. was supported
 366 by DFG grant Ru 1839/2-1. This is TRR 170 publication no. 187. We thank xxx and
 367 xxx.

368 Open Research

369 The data used for the discussion and figures is summarized in the supplementary
 370 material (Table S1-S3) and available in full at <https://doi.org/10.5281/zenodo.7691390>
 371 (Collinet et al., 2023)

372 References

- 373 Agee, C. B., Wilson, N. V., McCubbin, F. M., Ziegler, K., Polyak, V. J., Sharp,
 374 Z. D., ... Elardo, S. M. (2013). Unique Meteorite from Early Amazonian
 375 Mars: Water-Rich Basaltic Breccia Northwest Africa 7034. *Science*. doi:
 376 10.1126/science.1228858
- 377 Armytage, R. M., Debaille, V., Brandon, A. D., & Agee, C. B. (2018). A complex
 378 history of silicate differentiation of Mars from Nd and Hf isotopes in crustal
 379 breccia NWA 7034. *Earth and Planetary Science Letters*, 502, 274–283. doi:
 380 10.1016/j.epsl.2018.08.013
- 381 Baird, A. K., Toulmin, P., Clark, B. C., Rose, H. J., Keil, K., Christian, R. P., &
 382 Gooding, J. L. (1976). Mineralogic and petrologic implications of Viking geo-
 383 chemical results from Mars: Interim report. *Science*, 194(4271), 1288–1293.
 384 doi: 10.1126/science.194.4271.1288
- 385 Balta, J. B., & McSween, H. Y. (2013a). Application of the MELTS algo-
 386 rithm to Martian compositions and implications for magma crystalliza-
 387 tion. *Journal of Geophysical Research: Planets*, 118(12), 2502–2519. doi:
 388 10.1002/2013JE004461
- 389 Balta, J. B., & McSween, H. Y. (2013b). Water and the composition of Martian
 390 magmas. *Geology*. doi: 10.1130/g34714.1
- 391 Balta, J. B., Sanborn, M., McSween, H. Y., & Wadhwa, M. (2013). Magmatic his-
 392 tory and parental melt composition of olivine-phyric shergottite LAR 06319:
 393 Importance of magmatic degassing and olivine antecrysts in Martian magma-
 394 tism. *Meteoritics and Planetary Science*, n/a-n/a. doi: 10.1111/maps.12140
- 395 Baratoux, D., Toplis, M. J., Monnereau, M., & Gasnault, O. (2011). Thermal his-
 396 tory of Mars inferred from orbital geochemistry of volcanic provinces. *Nature*,

- 397 472(7343), 338–41. doi: 10.1038/nature09903
- 398 Barrat, J. A., Jambon, A., Bohn, M., Gillet, P., Sautter, V., Gopel, C., ... Keller,
399 F. (2002). Petrology and chemistry of the picritic shergottite North West
400 Africa 1068 (NWA 1068). *Geochimica Et Cosmochimica Acta*, 66(19), 3505–
401 3518.
- 402 Basu Sarbadhikari, A., Day, J. M., Liu, Y., Rumble, D., & Taylor, L. a. (2009). Pet-
403 rogenesis of olivine-phyric shergottite Larkman Nunatak 06319: Implications
404 for enriched components in martian basalts. *Geochimica et Cosmochimica
405 Acta*, 73(7), 2190–2214. doi: 10.1016/j.gca.2009.01.012
- 406 Bertka, C. M., & Fei, Y. (1997). Mineralogy of the Martian interior up to core-
407 mantle boundary pressures. *J. Geophys. Res.*, 102(B3), 5251–5264. doi: 10
408 .1029/96jb03270
- 409 Borgard, D. D., & Johnson, P. (1983). Martian gases in an antarctic meteorite? *Sci-
410 ence*, 221(4611), 651–654. doi: 10.1126/science.221.4611.651
- 411 Borg, L. E., & Draper, D. S. (2003). A petrogenetic model for the origin and compo-
412 sitional variation of the martian basaltic meteorites. *Meteoritics and Planetary
413 Science*, 38(12), 1713–1731.
- 414 Borg, L. E., Nyquist, L. E., Taylor, L. A., Wiesmann, H., & Shih, C. Y. (1997).
415 Constraints on Martian differentiation processes from Rb-Sr and Sm-Nd iso-
416 topic analyses of the basaltic shergottite QUE 94201. *Geochimica et Cos-
417 mochimica Acta*, 61(22), 4915–4931. doi: 10.1016/S0016-7037(97)00276-7
- 418 Bouvier, L. C., Costa, M. M., Connelly, J. N., Jensen, N. K., Wielandt, D., Storey,
419 M., ... Bizzarro, M. (2018). Evidence for extremely rapid magma ocean crys-
420 tallization and crust formation on Mars. *Nature*, 558(7711), 586–589. doi:
421 10.1038/s41586-018-0222-z
- 422 Brandon, A. D., Puchtel, I. S., Walker, R. J., Day, J. M., Irving, A. J., & Taylor,
423 L. a. (2012). Evolution of the martian mantle inferred from the 187Re–187Os
424 isotope and highly siderophile element abundance systematics of shergot-
425 tite meteorites. *Geochimica et Cosmochimica Acta*, 76, 206–235. doi:
426 10.1016/j.gca.2011.09.047
- 427 Cassata, W. S., Cohen, B. E., Mark, D. F., Trappitsch, R., Crow, C. A., Wimpenny,
428 J., ... Smith, C. L. (2018). Chronology of martian breccia NWA 7034 and
429 the formation of the martian crustal dichotomy. *Science Advances*, 4(5). doi:
430 10.1126/sciadv.aap8306
- 431 Collinet, M., Charlier, B., Namur, O., Oeser, M., Médard, E., & Weyer, S. (2017).
432 Crystallization history of enriched shergottites from Fe and Mg isotope frac-
433 tionation in olivine megacrysts. *Geochimica et Cosmochimica Acta*, 207,
434 277–297. doi: 10.1016/j.gca.2017.03.029
- 435 Collinet, M., Médard, E., Charlier, B., Vander Auwera, J., & Grove, T. L. (2015).
436 Melting of the primitive martian mantle at 0.5–2.2 GPa and the origin of
437 basalts and alkaline rocks on Mars. *Earth and Planetary Science Letters*,
438 427(0), 83–94. doi: <http://dx.doi.org/10.1016/j.epsl.2015.06.056>
- 439 Collinet, M., Plesa, A., Grove, T. L., Schwinger, S., Ruedas, T., & Breuer, D.
440 (2021). MAGMARS: A Melting Model for the Martian Mantle and FeO-Rich
441 Peridotite. *Journal of Geophysical Research: Planets*, 126(12), e2021JE006985.
442 doi: 10.1029/2021je006985
- 443 Collinet, M., Plesa, A.-C., Ruedas, T., Schwinger, S., & Breuer, D. (2023).
444 *The temperature and composition of the mantle sources of Martian basalts
445 [dataset+software]*. Zenodo. doi: 10.5281/zenodo.7691390
- 446 Condamine, P., & Médard, E. (2014). Experimental melting of phlogopite-bearing
447 mantle at 1 GPa: Implications for potassic magmatism. *Earth and Planetary
448 Science Letters*, 397(0), 80–92. doi: <http://dx.doi.org/10.1016/j.epsl.2014.04.027>
- 450 Costa, M. M., Jensen, N. K., Bouvier, L. C., Connelly, J. N., Mikouchi, T.,
451 Horstwood, M. S., ... Bizzarro, M. (2020). The internal structure and

- 452 geodynamics of Mars inferred from a 4.2-Gyr zircon record. *Proceedings of*
 453 *the National Academy of Sciences of the United States of America*, 117(49),
 454 30973–30979. doi: 10.1073/pnas.2016326117
- 455 Day, J. M. D., Tait, K. T., Udry, A., Moynier, F., Liu, Y., & Neal, C. R. (2018).
 456 Martian magmatism from plume metasomatized mantle. *Nature Communications*,
 457 9(1), 4799. doi: 10.1038/s41467-018-07191-0
- 458 Debaille, V., Yin, Q.-Z., Brandon, A., & Jacobsen, B. (2008). Martian mantle
 459 mineralogy investigated by the ^{176}Lu - ^{176}Hf and ^{147}Sm - ^{143}Nd systematics
 460 of shergottites. *Earth and Planetary Science Letters*, 269(1-2), 186–199. doi:
 461 10.1016/j.epsl.2008.02.008
- 462 Dreibus, G., & Wänke, H. (1985). Mars, a volatile-rich planet. *Meteoritics*, 20(2),
 463 367–381.
- 464 El Maarry, M., Gasnault, O., Toplis, M., Baratoux, D., Dohm, J., Newsom, H., ...
 465 Karunatillake, S. (2009). Gamma-ray constraints on the chemical composition
 466 of the martian surface in the Tharsis region: A signature of partial melting
 467 of the mantle? *Journal of Volcanology and Geothermal Research*, 185(1-2),
 468 116–122. doi: 10.1016/j.jvolgeores.2008.11.027
- 469 Elkins-Tanton, L. T., Hess, P. C., & Parmentier, E. M. (2005). Possible formation of
 470 ancient crust on Mars through magma ocean processes. *Journal of Geophysical
 471 Research: Planets*, 110(E12), E12S01. doi: 10.1029/2005JE002480
- 472 Elkins-Tanton, L. T., Parmentier, E. M., & Hess, P. C. (2003). Magma ocean
 473 fractional crystallization and cumulate overturn in terrestrial planets: Impli-
 474 cations for Mars. *Meteoritics and Planetary Science*, 38(12), 1753–1771. doi:
 475 10.1111/j.1945-5100.2003.tb00013.x
- 476 Farley, K. A., Stack, K. M., Shuster, D. L., Horgan, B. H. N., Hurowitz, J. A.,
 477 Tarnas, J. D., ... Zorzano, M.-P. (2022). Aqueously altered igneous rocks
 478 sampled on the floor of Jezero crater, Mars. *Science*, 0(0), eabo2196. doi:
 479 10.1126/science.abo2196
- 480 Ferdous, J., Brandon, A., Peslier, A., & Pirotte, Z. (2017). Evaluating Crustal Con-
 481 tributions to Enriched Shergottites from the Petrology, Trace Elements, and
 482 Rb-Sr and Sm-Nd Isotope Systematics of Northwest Africa 856. *Geochimica et
 483 Cosmochimica Acta*. doi: 10.1016/j.gca.2017.05.032
- 484 Filiberto, J. (2017). Geochemistry of Martian basalts with constraints on magma
 485 genesis. *Chemical Geology*, 466, 1–14. doi: <https://doi.org/10.1016/j.chemgeo.2017.06.009>
- 486 Filiberto, J., & Dasgupta, R. (2011). Fe $^{2+}$ -Mg partitioning between olivine and
 487 basaltic melts: Applications to genesis of olivine-phyric shergottites and condi-
 488 tions of melting in the Martian interior. *Earth and Planetary Science Letters*,
 489 304(3-4), 527–537. doi: 10.1016/j.epsl.2011.02.029
- 490 Filiberto, J., & Dasgupta, R. (2015). Constraints on the depth and thermal vigor
 491 of melting in the Martian mantle. *Journal of Geophysical Research: Planets*,
 492 2014JE004745. doi: 10.1002/2014JE004745
- 493 Filiberto, J., Dasgupta, R., Kiefer, W. S., & Treiman, A. H. (2010). High pressure,
 494 near-liquidus phase equilibria of the Home Plate basalt Fastball and melt-
 495 ing in the Martian mantle. *Geophysical Research Letters*, 37(13), 1–4. doi:
 496 10.1029/2010GL043999
- 497 Filiberto, J., Musselwhite, D. S., Gross, J., Burgess, K., Le, L., & Treiman, A. H.
 498 (2010). Experimental petrology, crystallization history, and parental magma
 499 characteristics of olivine-phyric shergottite NWA 1068: Implications for the
 500 petrogenesis of “enriched” olivine-phyric shergottites. *Meteoritics and Plane-
 501 tary Science*, 45(8), 1258–1270. doi: 10.1111/j.1945-5100.2010.01080.x
- 502 Filiberto, J., Treiman, A. H., & Le, L. (2008). Crystallization experiments on a Gu-
 503 sev Adirondack basalt composition. *Meteoritics and Planetary Science*, 43(7),
 504 1137–1146.
- 505 Goodrich, C. A., Treiman, A. H., Filiberto, J., Gross, J., & Jercinovic, M. (2013).

- 507 K₂O-rich trapped melt in olivine in the Nakhla meteorite: Implications for
 508 petrogenesis of nakhrites and evolution of the Martian mantle. *Meteoritics and*
 509 *Planetary Science*, 48(12), 2371–2405. doi: 10.1111/maps.12226
- 510 Greeley, R., Foing, B. H., McSween, H. Y., Neukum, G., Pinet, P., van Kan, M.,
 511 ... Zegers, T. E. (2005). Fluid lava flows in Gusev crater, Mars. *Journal of*
 512 *Geophysical Research E: Planets*, 110(5), 1–6. doi: 10.1029/2005JE002401
- 513 Greshake, A., Fritz, J., & Stöffler, D. (2004). Petrology and shock metamorphism of
 514 the olivine-phyric shergottite Yamato 980459: Evidence for a two-stage cooling
 515 and a single-stage ejection history. *Geochimica Et Cosmochimica Acta*, 68(10),
 516 2359–2377. doi: 10.1016/j.gca.2003.11.022
- 517 Gross, J., Treiman, A. H., Filiberto, J., & Herd, C. D. K. (2011). Primitive olivine-
 518 phyric shergottite NWA 5789: Petrography, mineral chemistry, and cooling
 519 history imply a magma similar to Yamato-980459. *Meteoritics and Planetary*
 520 *Science*, 133(1), no-no. doi: 10.1111/j.1945-5100.2010.01152.x
- 521 He, Q., Xiao, L., Hsu, W., Balta, J. B., McSween, H. Y., & Liu, Y. (2013). The
 522 water content and parental magma of the second chassignite NWA 2737: Clues
 523 from trapped melt inclusions in olivine. *Meteoritics and Planetary Science*,
 524 48(3), 474–492. doi: 10.1111/maps.12073
- 525 Huang, Q., Schmerr, N. C., King, S. D., Kim, D., Rivoldini, A., Plesa, A. C.,
 526 ... Banerdt, W. B. (2022). Seismic detection of a deep mantle discon-
 527 tinuity within Mars by InSight. *Proceedings of the National Academy*
 528 *of Sciences of the United States of America*, 119(42), e2204474119. doi:
 529 10.1073/pnas.2204474119
- 530 Humayun, M., Nemchin, A., Zanda, B., Hewins, R. H., Grange, M., Kennedy, A.,
 531 ... Deldicque, D. (2013). Origin and age of the earliest Martian crust from
 532 meteorite NWA 7533. *Nature*, 503(7477), 513–516. doi: 10.1038/nature12764
- 533 Johnston, D. H., & Toksöz, M. N. (1977). Internal structure and properties of Mars.
 534 *Icarus*, 32(1), 73–84. doi: 10.1016/0019-1035(77)90050-1
- 535 Katz, R. F., Spiegelman, M., & Langmuir, C. H. (2003). A new parameterization
 536 of hydrous mantle melting. *Geochemistry, Geophysics, Geosystems*, 4(9), 1073.
 537 doi: 10.1029/2002GC000433
- 538 Khan, A., Ceylan, S., van Driel, M., Giardini, D., Lognonné, P., Samuel, H., ...
 539 Banerdt, W. B. (2021). Upper mantle structure of Mars from InSight seismic
 540 data. *Science*, 373(6553), 434–438. doi: 10.1126/science.abf2966
- 541 Khan, A., Sossi, P. A., Liebske, C., Rivoldini, A., & Giardini, D. (2022). Geophys-
 542 ical and cosmochemical evidence for a volatile-rich Mars. *Earth and Planetary*
 543 *Science Letters*, 578, 117330. doi: 10.1016/j.epsl.2021.117330
- 544 Kruijer, T. S., Kleine, T., Borg, L. E., Brennecke, G. A., Irving, A. J., Bischoff,
 545 A., & Agee, C. B. (2017). The early differentiation of Mars inferred
 546 from Hf–W chronometry. *Earth and Planetary Science Letters*. doi:
 547 10.1016/j.epsl.2017.06.047
- 548 Lagain, A., Benedix, G. K., Servis, K., Baratoux, D., Doucet, L. S., Rajšić, A., ...
 549 Miljković, K. (2021). The Tharsis mantle source of depleted shergottites re-
 550 vealed by 90 million impact craters. *Nature Communications*, 12(1), 1–9. doi:
 551 10.1038/s41467-021-26648-3
- 552 Lagain, A., Bouley, S., Zanda, B., Miljković, K., Rajšić, A., Baratoux, D., ...
 553 Bland, P. A. (2022). Early crustal processes revealed by the ejection site
 554 of the oldest martian meteorite. *Nature Communications*, 13(1), 3782. doi:
 555 10.1038/s41467-022-31444-8
- 556 Lee, C.-T. A., Luffi, P., Plank, T., Dalton, H., & Leeman, W. P. (2009). Con-
 557 straints on the depths and temperatures of basaltic magma generation on
 558 Earth and other terrestrial planets using new thermobarometers for mafic
 559 magmas. *Earth and Planetary Science Letters*, 279(1–2), 20–33. doi:
 560 http://dx.doi.org/10.1016/j.epsl.2008.12.020
- 561 Lodders, K., & Fegley, B. (1997). An oxygen isotope model for the composition of

- Mars. *Icarus*, 126(2), 373–394. doi: 10.1006/icar.1996.5653
- Longhi, J., Knittle, E., Holloway, J. R., & Waenke, H. (1992). The bulk composition, mineralogy and internal structure of Mars. In *Mars* (pp. 184–208). AA(Lamont-Doherty Earth Observatory), AB(University of California, Santa Cruz), AC(Arizona State University), AD(Max-Planck-Institute for Chemistry, Mainz).
- Matzen, A. K., Woodland, A., Beckett, J. R., & Wood, B. J. (2022). Oxidation state of iron and Fe-Mg partitioning between olivine and basaltic martian melts. *American Mineralogist*, 107(7), 1442–1452. doi: 10.2138/am-2021-7682
- McCubbin, F. M., Boyce, J. W., Srinivasan, P., Santos, A. R., Elardo, S. M., Filiberto, J., ... Shearer, C. K. (2016). Heterogeneous distribution of H₂O in the Martian interior: Implications for the abundance of H₂O in depleted and enriched mantle sources. *Meteoritics and Planetary Science*, 51(11), 2036–2060. doi: 10.1111/maps.12639
- McCubbin, F. M., Elardo, S. M., Shearer, C. K., Smirnov, A., Hauri, E. H., & Draper, D. S. (2013). A petrogenetic model for the comagmatic origin of chassignites and nakhlites: Inferences from chlorine-rich minerals, petrology, and geochemistry. *Meteoritics and Planetary Science*, 48(5), 819–853. doi: 10.1111/maps.12095
- McFarlane, C. R. M., & Spray, J. G. (2022). The Los Angeles martian diabase: Phosphate U-Th-Pb geochronology and mantle source constraints. *Geochimica et Cosmochimica Acta*, 326, 166–179. doi: <https://doi.org/10.1016/j.gca.2022.04.006>
- McSween, H. Y., Ruff, S. W., Morris, R. V., Bell, J. F., Herkenhoff, K., Gellert, R., ... Schmidt, M. (2006). Alkaline volcanic rocks from the Columbia Hills, Gusev crater, Mars. *Journal of Geophysical Research E: Planets*, 111(9), n/a–n/a. doi: 10.1029/2006JE002698
- McSween, H. Y., Wyatt, M. B., Gellert, R., Bell, I. F., Morris, R. V., Herkenhoff, K. E., ... Zipfel, J. (2006). Characterization and petrologic interpretation of olivine-rich basalts at Gusev Crater, Mars. *Journal of Geophysical Research E: Planets*, 111(2), 1–17. doi: 10.1029/2005JE002477
- Ming, D. W., Gellert, R., Morris, R. V., Arvidson, R. E., Brückner, J., Clark, B. C., ... Zipfel, J. (2008). Geochemical properties of rocks and soils in Gusev Crater, Mars: Results of the Alpha Particle X-Ray Spectrometer from Cumberland Ridge to Home Plate. *Journal of Geophysical Research: Planets*, 113(E12), E12S39. doi: 10.1029/2008JE003195
- Misawa, K. (2004). The Yamato 980459 olivine-phyric shergottite consortium. *Antarctic Meteorite Research*, 17, 1–12.
- Monders, A. G., Médard, E., & Grove, T. L. (2007). Phase equilibrium investigations of the Adirondack class basalts from the Gusev plains, Gusev crater, Mars. *Meteoritics and Planetary Science*, 42(1), 131–148. doi: 10.1111/j.1945-5100.2007.tb00222.x
- Moser, D. E., Chamberlain, K. R., Tait, K. T., Schmitt, A. K., Darling, J. R., Barker, I. R., & Hyde, B. C. (2013). Solving the Martian meteorite age conundrum using micro-baddeleyite and launch-generated zircon. *Nature*, 499(7459), 454–457. doi: 10.1038/nature12341
- Musselwhite, D. S., Dalton, H. A., Kiefer, W. S., & Treiman, A. H. (2006). Experimental petrology of the basaltic shergottite Yamato-980459: Implications for the thermal structure of the Martian mantle. *Meteoritics and Planetary Science*, 41(9), 1271–1290. doi: 10.1111/j.1945-5100.2006.tb00521.x
- Nyquist, L. E., Shih, C. Y., McCubbin, F. M., Santos, A. R., Shearer, C. K., Peng, Z. X., ... Agee, C. B. (2016). Rb-Sr and Sm-Nd isotopic and REE studies of igneous components in the bulk matrix domain of Martian breccia Northwest Africa 7034. *Meteoritics and Planetary Science*, 51(3), 483–498. doi: 10.1111/maps.12606

- Ostwald, A., Udry, A., Payré, V., Gazel, E., & Wu, P. (2022). The role of assimilation and fractional crystallization in the evolution of the Mars crust. *Earth and Planetary Science Letters*, 585, 117514. doi: 10.1016/j.epsl.2022.117514
- Payré, V., Siebach, K. L., Dasgupta, R., Udry, A., Rampe, E. B., & Morrison, S. M. (2020). Constraining Ancient Magmatic Evolution on Mars Using Crystal Chemistry of Detrital Igneous Minerals in the Sedimentary Bradbury Group, Gale Crater, Mars. *Journal of Geophysical Research: Planets*, 125(8), e2020JE006467. doi: 10.1029/2020JE006467
- Peslier, A. H., Hnatyshin, D., Herd, C. D. K., Walton, E. L., Brandon, A. D., Lapen, T. J., & Shafer, J. T. (2010). Crystallization, melt inclusion, and redox history of a Martian meteorite: Olivine-phyric shergottite Larkman Nunatak 06319. *Geochimica et Cosmochimica Acta*, 74(15), 4543–4576. doi: 10.1016/j.gca.2010.05.002
- Plesa, A. C., Wieczorek, M., Knapmeyer, M., Rivoldini, A., Walterová, M., & Breuer, D. (2022). Interior dynamics and thermal evolution of Mars – a geodynamic perspective. In *Advances in geophysics* (Vol. 63, pp. 179–230). Elsevier. doi: 10.1016/bs.agph.2022.07.005
- Schmidt, M. E., Campbell, J. L., Gellert, R., Perrett, G. M., Treiman, A. H., Blaney, D. L., ... Wiens, R. C. (2014). Geochemical diversity in first rocks examined by the Curiosity Rover in Gale Crater: Evidence for and significance of an alkali and volatile-rich igneous source. *Journal of Geophysical Research: Planets*, n/a–n/a. doi: 10.1002/2013JE004481
- Schmidt, M. E., & McCoy, T. J. (2010). The evolution of a heterogeneous Martian mantle: Clues from K, P, Ti, Cr, and Ni variations in Gusev basalts and shergottite meteorites. *Earth and Planetary Science Letters*, 296(1-2), 67–77. doi: 10.1016/j.epsl.2010.04.046
- Shafer, J. T., Brandon, A. D., Lapen, T. J., Righter, M., Peslier, A. H., & Beard, B. L. (2010). Trace element systematics and 147Sm-143Nd and 176Lu-176Hf ages of Larkman Nunatak 06319: Closed-system fractional crystallization of an enriched shergottite magma. *Geochimica et Cosmochimica Acta*, 74(24), 7307–7328. doi: 10.1016/j.gca.2010.09.009
- Shih, C.-Y., Nyquist, L., Wiesmann, H., Reese, Y., & Misawa, K. (2005). Rb-Sr and Sm-Nd dating of olivine-phyric shergottite Yamato 980459: Petrogenesis of depleted shergottites. *Antarctic meteorite research*, 18, 46–65.
- Shirai, N., & Ebihara, M. (2004). Chemical characteristics of a Martian meteorite, Yamato 980459. *Antarctic Meteorite Research*, 17, 55–67.
- Smith, D., Griffin, W. L., & Ryan, C. G. (1993). Compositional evolution of high-temperature sheared lherzolite PHN 1611. *Geochimica et Cosmochimica Acta*, 57(3), 605–613. doi: 10.1016/0016-7037(93)90371-3
- Squyres, S. W., Aharonson, O., Clark, B. C., Cohen, B. a., Crumpler, L., de Souza, P. a., ... Yen, A. (2007). Pyroclastic activity at Home Plate in Gusev Crater, Mars. *Science*, 316(5825), 738–42. doi: 10.1126/science.1139045
- Symes, S. J. K., Borg, L. E., Shearer, C. K., & Irving, A. J. (2008). The age of the martian meteorite Northwest Africa 1195 and the differentiation history of the shergottites. *Geochimica et Cosmochimica Acta*, 72(6), 1696–1710. doi: 10.1016/j.gca.2007.12.022
- Udry, A., & Day, J. M. D. (2018). 1.34 billion-year-old magmatism on Mars evaluated from the co-genetic nakhlite and chassignite meteorites. *Geochimica et Cosmochimica Acta*, 238, 292–315. doi: 10.1016/j.gca.2018.07.006
- Udry, A., Gazel, E., & McSween, H. Y. (2018). Formation of Evolved Rocks at Gale Crater by Crystal Fractionation and Implications for Mars Crustal Composition. *Journal of Geophysical Research: Planets*, 123(6), 1525–1540. doi: 10.1029/2018JE005602
- Udry, A., Lunning, N. G., McSween Jr, H. Y., & Bodnar, R. J. (2014). Petrogenesis of a vitrophyre in the martian meteorite breccia NWA 7034. *Geochimica*

- 672 *et Cosmochimica Acta*, 141(0), 281–293. doi: <http://dx.doi.org/10.1016/j.gca.2014.06.026>
- 673 Wieczorek, M. A., Broquet, A., McLennan, S. M., Rivoldini, A., Golombek, M., Antonangeli, D., ... Banerdt, W. B. (2022). InSight Constraints on the Global Character of the Martian Crust. *Journal of Geophysical Research: Planets*, 127(5), 1–35. doi: 10.1029/2022JE007298
- 674 Wiens, R. C., Udry, A., Beyssac, O., Quantin-Nataf, C., Mangold, N., Cousin, A., ... Null, N. (2022). Compositionally and density stratified igneous terrain in Jezero crater, Mars. *Science Advances*, 8(34), eabo3399. doi: 10.1126/sciadv.abo3399
- 675 Wittmann, A., Korotev, R. L., Jolliff, B. L., Irving, A. J., Moser, D. E., Barker, I., & Rumble, D. (2015). Petrography and composition of Martian regolith breccia meteorite Northwest Africa 7475. *Meteoritics and Planetary Science*, 50(2), 326–352. doi: 10.1111/maps.12425
- 676 Wu, Y., Hsu, W., Li, Q.-L., Che, X., & Liao, S. (2021). Heterogeneous martian mantle: Evidence from petrology, mineral chemistry, and in situ U-Pb chronology of the basaltic shergottite Northwest Africa 8653. *Geochimica et Cosmochimica Acta*, 309, 352–365. doi: <https://doi.org/10.1016/j.gca.2021.05.011>
- 677 Yoshizaki, T., & McDonough, W. F. (2020). The composition of Mars. *Geochimica et Cosmochimica Acta*, 273, 137–162. doi: 10.1016/j.gca.2020.01.011
- 678
679
680
681
682
683
684
685
686
687
688
689
690
691

Figure 1.

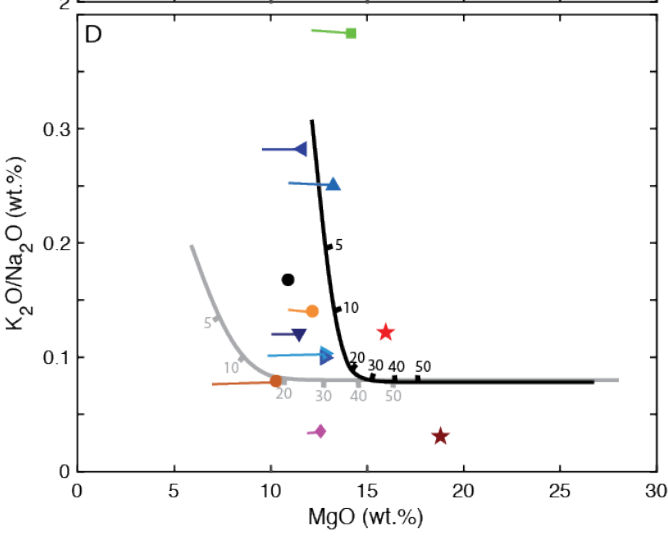
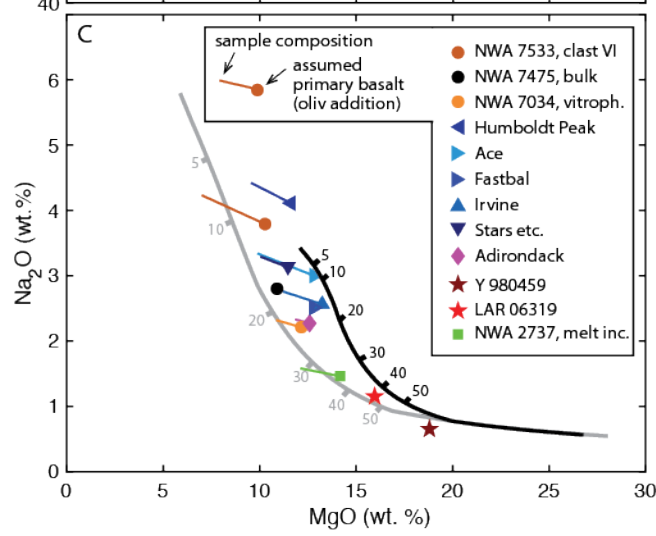
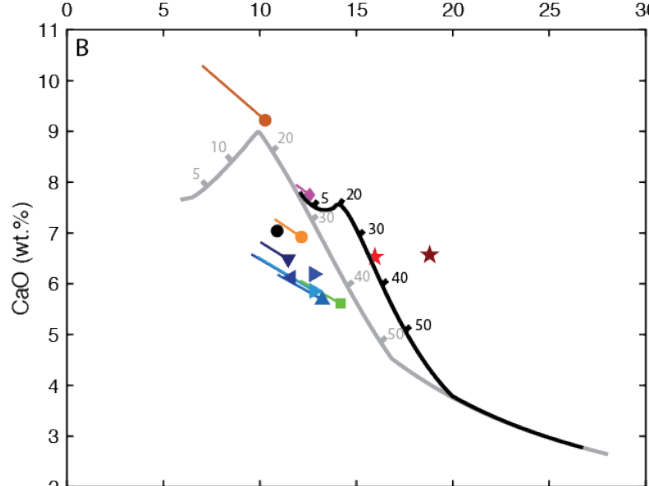
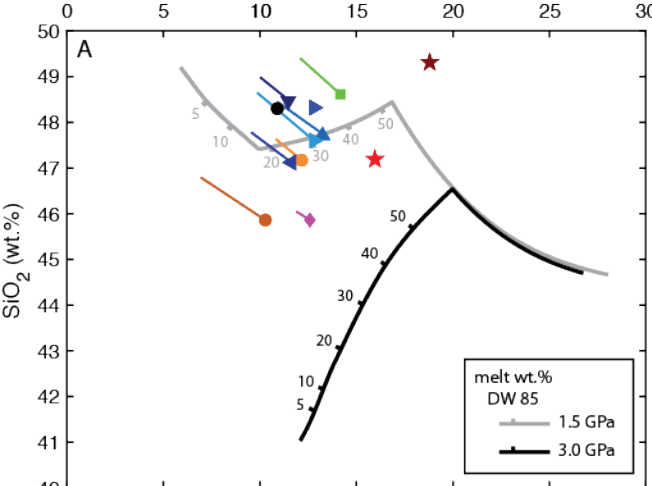


Figure 2.

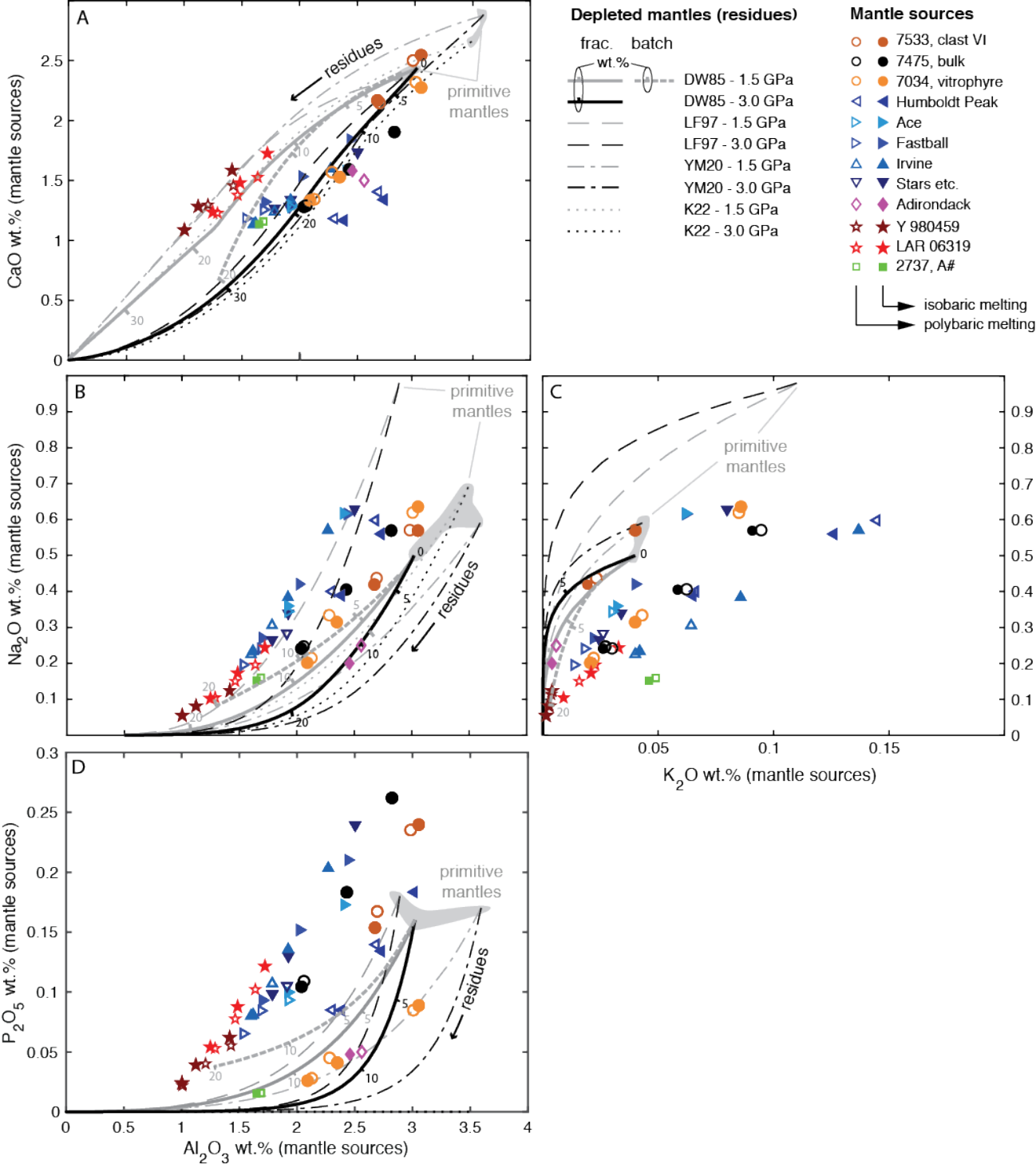


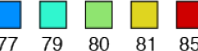
Figure 3.

thermochemical evolution model (Plesa et al., 2022):

— min. — max.

★ T_p at possible source locations
(Karratha, Gusev and 09-000015 craters)

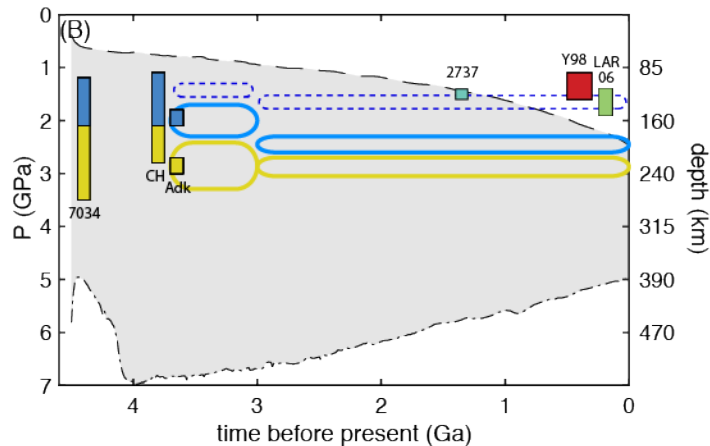
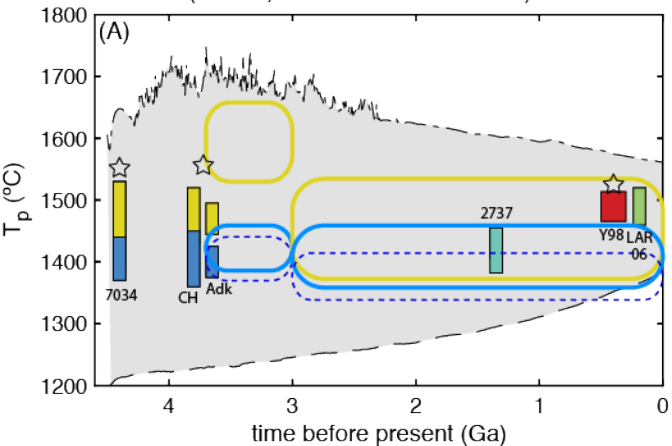
mantle Mg#



GRS

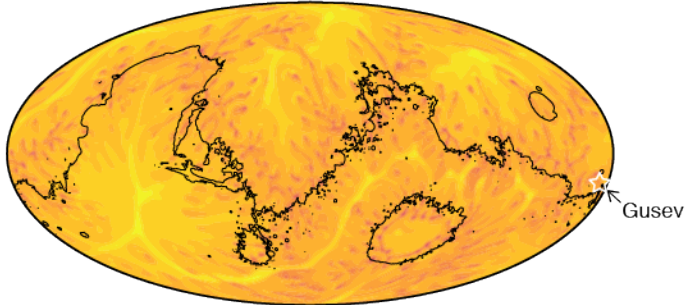
DW 85 YM 20 (MAGMARS)

DW 85 - Baratoux+2011 (pMELTS)



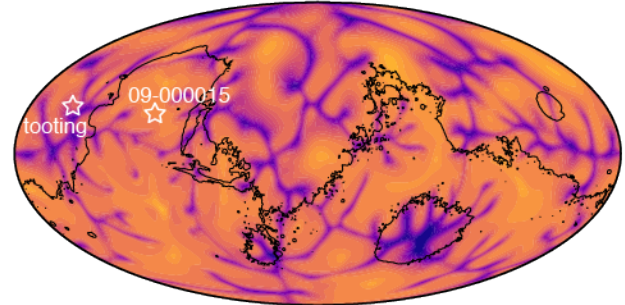
(C)

3.7 Ga



(D)

0.47 Ga



1250 1350 1450 1550 1650
 T_p - mantle potential temperature at 450 km (°C)